CENG0026 Coursework 1

Design Report

1 Introduction

Fuel cells (FCs) are an excellent choice for long-range heavy goods vehicles (HGVs), due to high energy densities, short refuelling times and better range capabilities than battery electric vehicles (BEVs), quieter operation and 0 emissions at the tailpipe compared to internal combustion engine (ICE) vehicles. Herein, we elucidate theoretical performance of a fuel cell hybrid electric vehicle (FCHEV) based on a class 8 semi-truck.

The maximum weight limit for heavy goods vehicles (HGVs) in the UK is 44,000 kg [1]. Rolling resistance constants for HGVs can range from 0.006 − 0.007 [2] with drivetrain efficiencies of up to 0.9 [3] possible for EVs. Drag coefficients and frontal areas vary from model to model. Here we use values representative of a Tesla Semi [4] which has a stated range of 500 miles.

$$\mathrm{M_v} = 44,000 \text{ kg}$$

$$\mathrm{f_r} = 0.007$$

$$\mathrm{C_d} = 0.36$$

$$\text{Range} = 500 \text{ miles}$$

$$\eta = 0.9$$

$$\mathrm{A_f} = 9.56 \text{ m}^2$$

$$\rho_\mathrm{a} = 1.225 \text{ kgm}^{-3}$$

$$\mathrm{g} = 9.81 \text{ ms}^{-2}$$

, where M_v = vehicle mass, f_r = rolling resistance constant, C_d = drag coefficient, η = drive train efficiency, A_f = frontal area, ρ_a = density of air and g = gravitational constant.

2 Power Cycle

Here, we use the United States Environmental Protection Agency (EPA) Heavy Duty Urban Dynamometer Driving Schedule [5] which is suitable for HGVs, shown in figure 1(a), to calculate a theoretical power cycle. The cycle covers a distance of 5.55 miles over a time of 20 minutes. The total resistance to vehicle motion, F_{vehicle}, travelling at velocity v is given by $F_{\text{vehicle}} = F_{\text{rolling}} + F_{\text{aero}} + F_{\text{acceleration}}$, where

$$\begin{aligned} F_{\text{rolling}} &= M_v g f_r \\ F_{\text{aero}} &= \frac{1}{2}\rho A_{\text{f}} C_d v^2 \\ F_{\text{acceleration}} &= M_{\text{v}} \frac{\text{dV}}{\text{dt}} \end{aligned}$$

The power required at the wheels is then given by $P_{\text{wheels}} = F_{vehicle} v$, and the power required at the prime mover, which for a FCHEV is an electric motor, is given by

$$P_{\text{mover}} = \frac{P_{\text{wheels}}}{\eta_t} \tag{1}$$

Equation 1 can then be used to obtain the power cycle, at the prime mover, shown in figures 1(a) and 1(b). If the vehicle employs regenerative braking (regen), where $P_{\text{mover}} < 0$, then a portion of the energy dissipated during braking is used to charge the battery, given by the regen factor α_{regen} ($\alpha = 0.4$ in this report) and shown in orange in figures 1(b) and 1(c). Figure 1(d) shows the cumulative energy usage over a single drive cycle with a total energy output $E_{\text{mover}} = 22.68$ kWh, with $E_{\text{regen}} = 4.9$ kWh regenerated, thereby consuming a total of $E_{\text{total}} = 17.78$ kWh of energy to travel 5.55 miles, giving an energy consumption of 3.2 kWh/mile; notably higher than the claimed < 2 kWh/mile of the (36,000kg when fully loaded) Tesla Semi. The average power the prime mover needs to provide is $P_{\text{avg}} = 76.9$ kW with a peak power output of $P_{\text{peak}} = 832$ kW required.

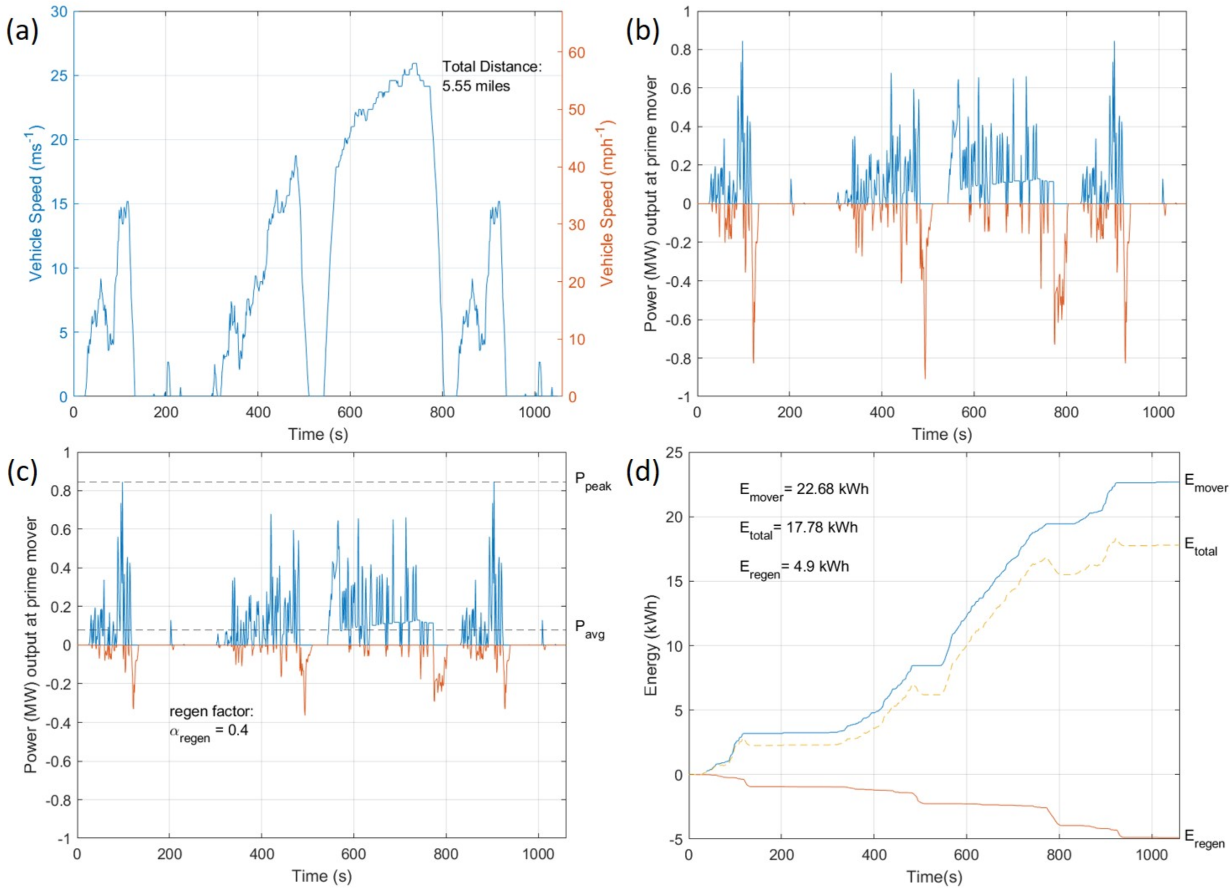

Figure 1: (a) EPA Heavy Duty Urban Drive Cycle with a total distance of 5.55 miles covered, (b) Power cycle at prime mover without regen, (c) Power cycle at prime mover with a regen-factor of $\alpha = 0.4$ with P_{avg} and P_{peak} indicating the average and peak power requirements, and (d) cumulative energy usage over the cycle with the blue line showing energy provided by prime mover and orange line showing regenerated energy and dotted yellow line showing total consumed energy

3 Hybridisation

A series architecture [6], shown in figure 2, allows both the FC and the battery to power the vehicle as well as allowing power regenerated through braking to charge the battery, making it suitable for FCHEVs.

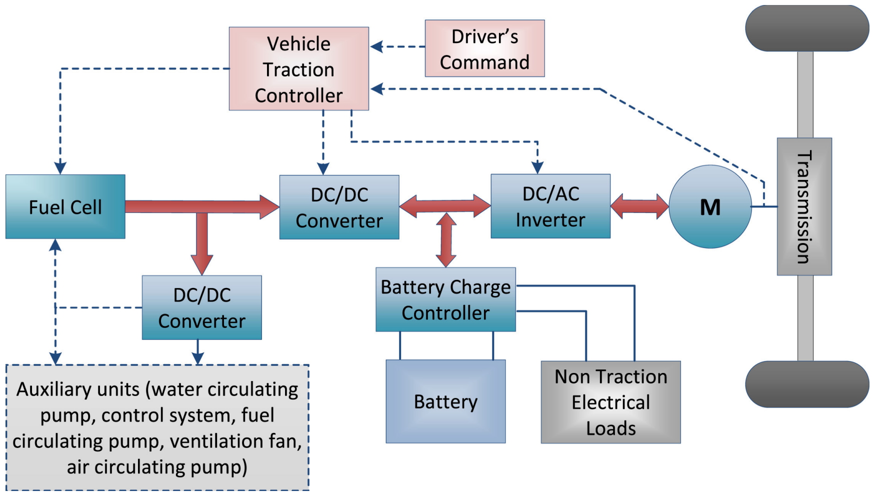

Figure 2: A FCHEV series architecture where power to the wheels is delivered via an electric motor. The motor takes power from both the fuel cell and a battery. The battery can also be charged during braking

4 Sizing

During vehicle operation, power requirements will move above and below the fuel cell's constant output P_{avg}. To handle this dynamic load, when power requirement $P_{\text{rq}} > P_{\text{avg}}$, the battery makes up the difference providing a power $P_{\text{bat}} = P_{\text{rq}} - P_{\text{avg}}$. When $P_{\text{rq}} < P_{\text{avg}}$ but above 0, the fuel cell is still operated at constant load and the difference $P_{\text{avg}} - P_{\text{rq}}$ is used to charge the battery. Finally, when $P_{\text{rq}} < 0$ i.e. the vehicle is braking, a fraction given by the regen factor α, is used to charge the battery.

Figure 3 shows the cumulative battery energy draw over a single cycle, where a positive gradient indicates energy charge and a negative gradient energy discharge.The minimum value represents the maximum amount of energy that had been drawn during a single cycle, here a value of 8.19 kWh. For a range of 500 miles this equates to 737.13 kWh of battery capacity needed.

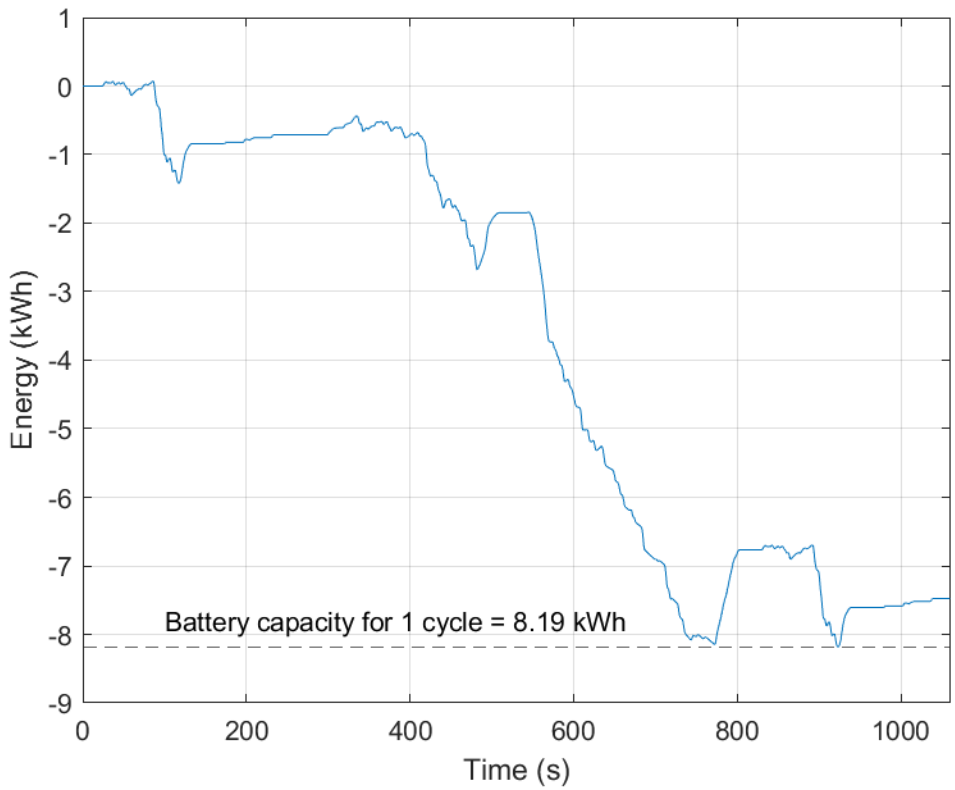

Figure 3: Energy draw on battery over a single drive cycle. The minimum point is used to estimate battery capacity needed to drive a single drive cycle shown by the dotted line

5 Fuel and Fuel Cell Type

Polymer electrolyte membrane (PEMs) FC that use Hydrogen fuel and a polymer electrolyte operating < 80 °C are excellent for use in vehicles. The most common PEM is perfluorosulfonic acid with long side-chains that can be customised. Pt nanoparticles in carbon supports are an excellent FC catalyst [7].

Graphite treated with hydrophobic agents such as polytetrafluoroethylene (PTFE) or Teflon is a suitable gas diffusion layer material, due to its light weight, porous structure and good water ejection properties.

Pertinent choices for bipolar plates include metal, graphite and composite materials. Poor mechanical strength of composite and graphite materials make them unsuitable for use in HGVs. Poor corrosion resistance of metals, that otherwise display high mechanical strength and good electrical and thermal conductivity, will require frequent maintenance when use in a FCHEV. However, rapid progress is being made on corrosion-resistance surface treatments [8] for metals. Stainless steel (SS) metal plates can be made ultra-thin (0.1 mm) [8], are lightweight and cost-effective to mass-produce, and offer improved corrosion resistance after surface treatments; therefore making them a suitable material for use as bipolar plates in FCHEVs.

6 Modelling the Fuel Cell

The maximum expected voltage for an electron-carrying system in standard conditions is given by

$$E^0 = \frac{\triangle H - T\triangle S}{nF} \tag{2}$$

, where $\triangle H$ is the change in enthalpy, $\triangle S$ is the change in entropy, T is temperature, n is the number of electrons and F is the Faraday constant given $F = 96,485\ \mathrm{C} \cdot \mathrm{mol}^{-1}$. For a reversible adiabatic system i.e. where $\triangle S = 0$, the thermal voltage is given by

$$E^{00} = \frac{-\triangle H}{nF} \tag{3}$$

For a FC operating at T = 353 K, $\triangle H$ is given by

$$\begin{aligned} \triangle H = &\left(\bar{h}_{\mathrm{f,H_2O}} + \int_{T_{\mathrm{ref}}=298}^{T=353} \bar{c}_{p,\mathrm{H_2O}}(T)\,dT\right)_{\mathrm{H_2O}} - \frac{1}{2}\left(\bar{h}_{\mathrm{f,O_2}} + \int_{T_{\mathrm{ref}}=298}^{T=353} \bar{c}_{p,\mathrm{O_2}}(T)\,dT\right)_{\mathrm{O_2}} \\ &- \left(\bar{h}_{\mathrm{f,H_2}} + \int_{T_{\mathrm{ref}}=298}^{T=353} \bar{c}_{p,\mathrm{H_2}}(T)\,dT\right)_{\mathrm{H_2}} \end{aligned} \tag{4}$$

, and $\triangle S$ is given by

$$\begin{aligned} \triangle S = &\left(\bar{s}_{\mathrm{f,H_2O}} + \int_{T_{\mathrm{ref}}=298}^{T=353} \frac{\bar{c}_{p,\mathrm{H_2O}}}{T}(T)\,dT\right)_{\mathrm{H_2O}} - \frac{1}{2}\left(\bar{s}_{\mathrm{f,O_2}} + \int_{T_{\mathrm{ref}}=298}^{T=353} \frac{\bar{c}_{p,\mathrm{O_2}}}{T}(T)\,dT\right)_{\mathrm{O_2}} \\ &- \left(\bar{s}_{\mathrm{f,H_2}} + \int_{T_{\mathrm{ref}}=298}^{T=353} \frac{\bar{c}_{p,\mathrm{H_2}}}{T}(T)\,dT\right)_{\mathrm{H_2}} \end{aligned} \tag{5}$$

Taking values of average specific heats and entropy at 325 K, from the NIST Chemistry Webbook [9] to be $\bar{h}_{\mathrm{f,H_2O}} = 33.7$ kJmol^{-1}, $\bar{h}_{\mathrm{f,H_2}} = 28.9$ kJmol^{-1} and $\bar{h}_{\mathrm{f,O_2}} = 29.5$ kJmol^{-1} gives $\triangle H = -242,320$ kJ; and average specific entropy to be $\bar{s}_{\mathrm{f,H_2O}} = 0.188$ kJmol^{-1}K,

$\bar{s}_{\mathrm{f,O_2}} = 0.205$ kJmol^{-1}K and $\bar{s}_{\mathrm{f,H_2}} = 0.131$ kJmol^{-1}K gives $\triangle S = -46.1$ kJK^{-1}. Using equation 2 this gives a maximum expected voltage of $E_0 = 1.171$ V. For a system in non-standard conditions, the Nernst potential gives the open-circuit voltage

$$E_{OC} = E^0 + \frac{RT}{nF} \ln \frac{\prod a_{reactants}^{v_i}}{\prod a_{products}^{v_i}} \tag{6}$$

where the activity a_i is given by

$$a_i = \frac{P}{P_0} y_i$$

Using equation 6, typical pressures [10] of 3 atm at the cathode and 2 atm at the anode with mole fractions $y_{\mathrm{H_2}} = 0.8$ and $y_{\mathrm{O_2}} = 0.15$ gives an open-circuit voltage of $E_{\mathrm{OC}} = 1.171 + 0.00792 = 1.179$ V. Cells operating in real conditions, however, are subject to various activation (η_{act}), resistive (η_{ohmic}) and fuel utilisation (η_{conc}) losses and so the operating voltage of a practical fuel cell is given by $E_{cell} = E^0 - \eta_{act} - \eta_{ohmic} - \eta_{conc}$, where

$$\eta_{act} = -\frac{RT}{\alpha nF} \ln j_0 + \frac{RT}{\alpha nF} \ln j$$
$$\eta_{ohmic} = j \mathrm{ASR}_{\mathrm{ohmic}}$$
$$\eta_{conc} = c \ln \frac{j_L}{j_L - j}$$

Using

$$\mathrm{ASR}_{\mathrm{ohmic}} = 0.01\ \Omega\mathrm{cm}^{-2}$$
$$j_0^{H_2} = 0.1\ \mathrm{Acm}^{-2}$$
$$j_0^{O_2} = 10^{-4}\ \mathrm{Acm}^{-2}$$
$$\alpha_{\mathrm{H_2}} = 0.5$$
$$\alpha_{\mathrm{O_2}} = 0.3$$
$$j_{\mathrm{L}} = 2\ \mathrm{Acm}^{-2}$$
$$c = 0.1$$

and evaluating E_{cell} between $j = 0 - 2$ Acm^{-2} gives a polarisation curve shown in figure 4(a). Figure 4(b) shows the electric power density $P_{\mathrm{electric}} = jE_{\mathrm{cell}}$ (in orange) and waste heat density $P_{\mathrm{heat}} = j(E^{00} - E_{\mathrm{cell}})$ (in red) generated. Here, an operating point of V = 0.6

is used. The corresponding operating current density is 0.8 Acm^{-2}, giving a power density of $P_{\text{FC}} = 0.48\ \text{Wcm}^{-2}$

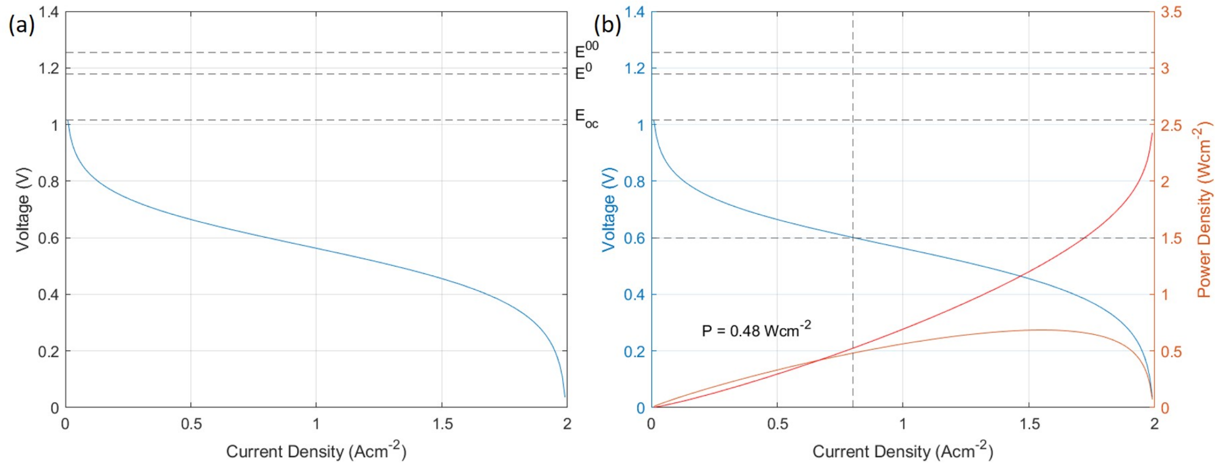

Figure 4: (a) Polarisation curve of the system with voltage and current density and (b) polarisation curve in blue, wasted heat density in red electric power density in orange with dotted lines at V = 0.6 and j = 0.8 Acm^{-2} used for this report generating a power density of 0.48 Wcm^{-2}

7 Physical Size of Fuel Cell

The FC needs to provide a constant power $P_{\text{avg}} = 76.9$ kW which gives an active FC electrode area of $\frac{P_{\text{avg}}}{P_{\text{FC}}} = 25.65\ \text{m}^2$. However high performance SS bipolar plates can have active areas of only 44% [8], translating into an actual cell area of 36.43 m^2. Several of these cells can be stacked to create a FC stack. For a constant power output, increasing the number of cells reduces the size of each cell, increases overall stack voltage and reduces the current that each cell outputs but also increases the weight of the stack.

Here we use a stack of 370 cells with each cell operating at 0.6 V, resulting in a voltage of 222 V, and an active single cell electrode area of 433 cm^2 with a total single cell area of 985 cm^2.

Using a SS bipolar plate with thickness 0.1 mm, mass 45 g [8] and single cell area of 985 cm^2 yields a fuel cell volume of 7.29 litres and mass 25.9 kg, relatively small when compared to a conventional class 8 diesel engine.

8 Reactant Flow Rate

Using Faraday's law $\dot{Q} = nF\dot{N}$ and a current density of 0.8 Acm^{-2} over an active electrode area of 433 cm^2 gives the flow rate of H_2 and O_2 as

$$\dot{N}_{\mathrm{H}_2} = 1.8 \times 10^{-3} \text{ mol} \cdot \text{s}^{-1} \quad \text{or} \quad 3.6 \times 10^{-3} \text{ g} \cdot \text{s}^{-1}$$
$$\dot{N}_{\mathrm{O}_2} = 8.9806 \times 10^{-4} \text{ mol} \cdot \text{s}^{-1} \quad \text{or} \quad 2.87 \times 10^{-2} \text{ g} \cdot \text{s}^{-1}$$

9 System Efficiency

The electrical power generated by our system is $P_e = jAE_{\mathrm{cell}}$, with a waste heat $P_{\mathrm{H}} = jA(E^{00} - E_{\mathrm{cell}})$, as shown in figure 4(a), giving an electrical efficiency of

$$\eta_{\mathrm{eff}} = \frac{P_e}{P_e + P_{\mathrm{H}}}$$

Here our FC generates an electrical power $P_e = 76.95$ kW with waste heat $P_{\mathrm{H}} = 84.09$ kW, returning an electrical efficiency of $\eta_{\mathrm{eff}} = 0.48$.

10 Battery Technology

Tesla currently uses Panasonic's 18650B lithium-ion cells [11] in its EVs. The cells have a gravimetric energy density of 243 Wh/kg and a volumetric energy density of 676 Wh/l, with a single cell energy capacity of 12.2 Wh, mass 46 g and volume 16.6 cm^3. Here, we use the same cells for our analysis.

In order to satisfy our energy capacity requirement of 737.13 kWh, we require 60,421 cells, necessitating a total volume of 1003 litres with a mass of 2779 kg. The cells have a peak current of 6.8 A with a voltage of 3.7 V, resulting in a peak power output of 25.16 W per cell. The total peak power output of our battery pack is 1.5 MW, more than enough for our peak power requirement of 832 kW.

With the FC weighing 25.9 kg and the battery pack weighing 2779 kg, the dry weight of our class 8 FCHEV is 14,145 kg, leaving 29,855 kg for cargo, which is about the same as a conventional diesel truck.

References

[1] G. D. for Transport. (). Accessed: March 4, 2021, [Online]. Available: `https://www.gov.uk/government/publications/hgv-maximum-weights/hgv-maximum-weights`.

[2] G. Paterlini and S. Yucel, "Rolling resistance validation," *Minnesota Department of Transportation, Tech. Rep*, 2015.

[3] S. Karlsson and D. Kushnir, "How energy efficient is electrified transport?," 2013.

[4] airshaper, "Tesla-semi concept simulation," 2018-09-12, Accessed : March 4, 2021. [Online]. Available: `https://airshaper.com/assets/reports/tesla_semi.pdf`.

[5] epa.gov. (). Accessed: March 4, 2021, [Online]. Available: `https://www.epa.gov/vehicle-and-fuel-emissions-testing/dynamometer-drive-schedules`.

[6] H. S. Das, C. W. Tan, and A. Yatim, "Fuel cell hybrid electric vehicles: A review on power conditioning units and topologies," *Renewable and Sustainable Energy Reviews*, vol. 76, pp. 268–291, 2017.

[7] Y. Prykhodko, K. Fatyeyeva, L. Hespel, and S. Marais, "Progress in hybrid composite nafion®-based membranes for proton exchange fuel cell application," *Chemical Engineering Journal*, p. 127 329, 2020.

[8] S. Haase, M. Moser, J. A. Hirschfeld, and K. Jozwiak, "Current density and catalyst-coated membrane resistance distribution of hydro-formed metallic bipolar plate fuel cell short stack with 250 cm2 active area," *Journal of Power Sources*, vol. 301, pp. 251–260, 2016.

[9] NIST. (). Accessed: March 4, 2021, [Online]. Available: `https://webbook.nist.gov/`.

[10] M. Ay, A. Midilli, and I. Dincer, "Exergetic performance analysis of a pem fuel cell," *International journal of energy research*, vol. 30, no. 5, pp. 307–321, 2006.

[11] O. LLC. (). Accessed: March 4, 2021, [Online]. Available: `https://www.orbtronic.com/batteries-chargers/panasonic-3400mah-18650-li-ion-battery-cell-ncr18650b`.